

Stability Indicating Method for a Thiazolyhydrazone Derivative with Antifungal Activity and Experimental/Theoretical Elucidation of Its Degradation Products

Iara R. Silva,^a Vinícius G. Maltarollo,^a Ícaro F. Protti,^a Renata B. Oliveira^a and Isabela C. César^{✉*,a}

^aDepartamento de Produtos Farmacêuticos, Faculdade de Farmácia, Universidade Federal de Minas Gerais, Av. Presidente Antônio Carlos, 6627, Pampulha, 31270-901 Belo Horizonte-MG, Brazil

RN104 (2-[2-(cyclohexylmethylene)hydrazinyl]-4-phenylthiazole) is a thiazolyhydrazone derivative with promising *in vitro* and *in vivo* antifungal activity. A stability indicating high-performance liquid chromatography with diode-array detection (HPLC-DAD) method was carried out using C18 end-capped column (250 × 4.6 mm, 5 μm) and a mobile phase composed of water and acetonitrile (15:85 v/v) at a flow rate of 1.2 mL min⁻¹, injection volume 25 μL and DAD detection at 240 nm. The method showed to be selective, linear in the range of 20 to 240 μg mL⁻¹, precise, accurate and robust. RN104 forced degradation study under different stress conditions (acidic, alkaline and neutral hydrolysis, oxidation, photolysis and thermolysis) was performed using the validated analytical method. The results showed that RN104 underwent significant degradation when subjected to alkaline hydrolysis and oxidation by metallic ions. Quantum mechanics calculations were carried out to assist in the structural elucidation of the formed degradation products. The obtained data may be useful for the development of future formulation based on RN104.

Keywords: stability indicating method, HPLC, forced degradation, quantum mechanics calculations

Introduction

A limited therapeutic arsenal is currently available for the treatment of fungal infections, mainly for immunocompromised patients. In addition, the incidence of fungal resistance to conventional drug has become a challenge for the health system.¹ Therefore, the development of new antifungal drugs more effective, safe and active against resistant strains is highly relevant.² In this context, a series of thiazolyhydrazone derivatives was developed by our group, and among them, the compound 2-[2-(cyclohexylmethylene)hydrazinyl]-4-phenylthiazole (RN104) (Figure 1) displayed clinically relevant *in vitro* and *in vivo* activity against fungi of the genera *Cryptococcus* spp. and *Candida* spp.³⁻⁵

Results of antibiofilm activity demonstrated that RN104 was effective in reducing biofilm formation by cryptococcal species and *Candida albicans*. RN104 was also able to interfere with adhesion capacity of *Candida*

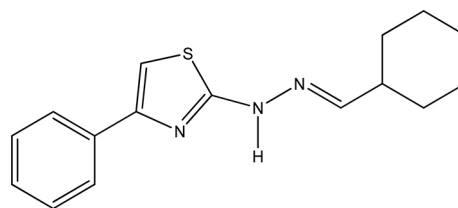


Figure 1. RN104 chemical structure.

yeasts to human buccal epithelial cells. In addition to *in vitro* models, RN104 was evaluated in the invertebrate models using *Galleria mellonella* larvae infected with *Cryptococcus gattii*, *Cryptococcus neoformans* or *C. albicans* and in cryptococcal murine model of infection. RN104 at dose of 5 mg kg⁻¹ significantly prolonged survival of infected larvae and at the dose of 10 mg kg⁻¹ per day over 15 days was as effective as fluconazole in prolonging the survival of mice infected with *C. gattii* and *C. albicans*.⁵ In a preclinical pharmacokinetic study in mice,⁶ RN104 was rapidly absorbed, reaching the maximum plasmatic concentration 20 min after administration. The bioavailability of *per os* route was approximately 40% of the intraperitoneal route.⁶

*e-mail: isacesar@gmail.com

Editor handled this article: Eduardo Carasek

The acute toxicity of the RN104 was evaluated and no mortality or toxic effect was observed in mice treated at dose of 300 mg kg⁻¹.⁷ Thus, considering the promising results displayed by RN104, the evaluation of the physicochemical characteristics and stability are important to confirm its potential as a possible drug candidate. The stability study performed for a drug candidate is a key step in the research and development of new drugs.^{8,9} The obtained results from stability studies have predictive potential in pharmacotechnical development; besides indicate the formation of possible toxic degradation products (DP) and the ideal storage conditions for the new drug.⁸

For the development of a stability indicating method, the exposure of the drug to different forced degradation conditions, such as photolysis, thermolysis, oxidation, and hydrolysis, is required by regulatory agencies worldwide.⁹⁻¹¹ For these studies, high performance liquid chromatography (HPLC) is the most recommended technique, due its high sensitivity and specificity.¹²

The identification of DP is a complementary study and provides a deep understanding regarding the pharmacological and toxicological impacts of the drug degradation. Quantum mechanics calculations (QMC) is a useful tool to predict the degradation pathways and the chemical structures of the DP formed in different conditions. QMC approach may support experimental data by calculating the reaction energy using statistical thermodynamics.¹³

Hence, the aims of this study were to develop and validate a stability-indicating method by high-performance liquid chromatography with diode-array detection (HPLC-DAD) and to evaluate the stability of RN104 in a forced degradation study under different conditions (acidic, alkaline and neutral hydrolysis, oxidation, photolysis and thermolysis). In addition, we proposed the chemical structures of the DP formed in the forced degradation studies.

Experimental

Instrumentation and reagents

HPLC analyses were carried out on an Agilent® 1100 series HPLC-DAD (Agilent® Technologies, Santa Clara, CA, USA) system composed of a quaternary pump, an on-line degasser, an auto sampler, a column oven and a diode array detector (DAD) with data acquisition from ChemStation software (Agilent Technologies, Santa Clara, CA, USA). A Nucleodur C18 end-capped column (250 × 4.6 mm, 5 μm) (Macherey-Nagel, Düren, Germany), kept at 30 °C was used. The mobile phase was composed of acetonitrile (Merck, LiChrosolv-Merck, Germany) and water (ultra-pure water was prepared from a Milli-Q

water purification system from Millipore, Bedford, MA, USA) (85:15 v/v), at a flow rate of 1.2 mL min⁻¹. The injection volume was 25 μL and detection was performed at 240 nm.

RN104 was synthesized in-house at the Laboratório de Química Farmacêutica of Faculdade de Farmácia (UFMG), as previously described by our group (purity 97.1%).⁴ Ultra-pure water was obtained from a Millipore system (Bedford, MA, USA). Acetonitrile and methanol (HPLC grade) were purchased from Merck (LiChrosolv-Merck, Darmstadt, Germany). All other chemicals used in the study, sodium hydroxide (NaOH, Synth, Diadema, SP, Brazil), hydrochloric acid (HCl, Neon, Suzano, SP, Brazil), hydrogen peroxide (H₂O₂, Supelco, Darmstadt, Germany) and ferric chloride (FeCl₃, Synth, Diadema, SP, Brazil) were of analytical grade.

Method validation

RN104 stock solution was prepared by weighing 25 mg of the compound and transferring to a 25 mL volumetric flask. The volume was completed with acetonitrile, so a 1 mg mL⁻¹ solution was obtained. The stock solution was diluted with mobile phase for the construction of the calibration curve and six different concentrations were prepared, corresponding to 20, 60, 100, 140, 180 and 240 μg mL⁻¹ of RN104. Three calibration curves for concentration *versus* peak area were plotted and the obtained data were subjected to regression analysis using the ordinary least squares method (OLSM). Peak areas of *E* isomer of RN104 were considered for method validation. The linearity was evaluated by means of coefficient of determination (r²) and coefficient of correlation (r).¹⁴ Analysis of variance (ANOVA) was used to verify the significance of regression and the deviation from linearity (α = 0.05).¹⁵

Intra-day and inter-day precisions were evaluated by the proximity between the results of the six replicates at 100% of nominal concentration (200 μg mL⁻¹), individually prepared and injected in triplicate. In the intra-day precision, the samples were prepared by the same analyst and analyzed in the same analytical run (n = 6). Inter-day precision differs from the previous test since the samples were prepared by different analysts, on two different days (n = 12). RN104 concentrations were determined and the relative standard deviation (RSD) was calculated.¹⁴

The accuracy was verified by nine determinations within the linear range, with three replicates of each concentration: 20, 120 and 240 μg mL⁻¹ (10, 60 and 120% of the nominal concentration, respectively).¹⁴ At each level, samples were prepared and the recovery percentage was determined.¹⁶

The limits of detection (LOD) and quantification (LOQ) of RN104 were expressed by the equations obtained from parameters of the analytical curve. From the calculated values, the experimental determination of LOQ and LOD was performed based on the signal-to-noise ratio. Diluted solutions of RN104 were prepared and injected in the chromatographic system, at decreasing concentrations. For the LOQ, the signal-to-noise ratio should be 10:1, whereas for LOD is 3:1.¹⁴

The selectivity of the method was tested by the evaluation of the spectral purity analysis of RN104 peak (240 $\mu\text{g mL}^{-1}$) by means of the diode array detector (DAD). In addition, solutions of RN104 at 200 $\mu\text{g mL}^{-1}$, RN103 (synthesis intermediate) and 2-bromoacetophenone (reagent used in synthesis) at 20 $\mu\text{g mL}^{-1}$ were injected in the HPLC system, isolated and simultaneously.¹⁴

In order to carry out the robustness evaluation, variations were introduced on the analytical parameters, using Youden test. RN104 sample solutions (200 $\mu\text{g mL}^{-1}$) were prepared and analyzed under the established conditions for the method and the following variation of the analytical parameters were analyzed: detector wavelength (260 nm), oven temperature (35 °C), mobile phase flow rate (1.0 mL min^{-1}), mobile phase composition (ACN:H₂O; 80:20), brand of the chromatographic column, brand of acetonitrile and chromatograph model.^{14,17}

Forced degradation study

The intrinsic stability of RN104 was evaluated by submitting the compound to several stress conditions, as established by international guidelines.^{9,11,12,18} To prepare the stock solution of RN104, about 20 mg of the compound was weighed and transferred to a 50 mL volumetric flask and the volume of the flask was completed with acetonitrile, resulting in a 400 $\mu\text{g mL}^{-1}$ solution. An aliquot of 5 mL of the stock solution of RN104 was transferred to a 10 mL volumetric flask, and the volume was completed with the appropriate diluent, resulting in a 200 $\mu\text{g mL}^{-1}$ solution. The diluents used for each degradation condition were 2 M HCl solution (acid hydrolysis), 2 M NaOH solution (alkaline hydrolysis), ultrapure water (neutral hydrolysis), 0.6% v/v H₂O₂ solution (oxidation) and 0.02 M FeCl₃ solution (oxidation by metal ions). The final volume of the volumetric flask was divided into two round-bottom glass tubes with lid, the first one was conditioned at room temperature (23 °C) and the second one stored in an oven at 50 °C, both protected from light. For each condition, blank solutions were also analyzed, keeping the same storage conditions of the tested samples. Aliquots of blank and test tubes were analyzed after 0, 24, 48 and 72 h. To obtain the

UV-Vis absorption spectrum of possible complex formed between Fe^{III} ion with RN104, the degradation reaction was repeated in the same conditions described above. At the end of the reaction, the solvent mixture was allowed to evaporate in a 10 mL headspace vial, to give a reddish brown residue that was used without purification. Then, the experimental UV-Vis spectrum in scan mode of residue and RN104 solutions in acetonitrile at 0.02 mg mL^{-1} was performed.

For the dry heat tests, about 1.0 mg of RN104 was exactly weighed in a watch glass. The glasses were covered with foil and stored in the oven at 105 °C. After 24, 48 and 72 h, each sample was diluted with 5 mL of mobile phase and analyzed. For the photodegradation test, the accurately weighed samples (about 1.0 mg) were packed in small glass tubes and transferred to the photodegradation chamber (1.2 million lux h^{-1} (visible light) and 200 W $\text{h}^{-1} \text{m}^{-2}$ (UV)).¹⁸ After 24, 48 and 72 h, samples were diluted with 5 mL of mobile phase and analyzed.

After the evaluation of the initial results of forced degradation tests, a degradation kinetic study for the conditions that presented considerable degradation was carried out, in milder conditions, and aliquots were withdrawn every hour, for 12 h. For this kinetic study, the concentration of RN104 in the stock solution was maintained, reducing the concentrations of degradation agent and the exposure time (72 to 12 h) in each condition: 0.2 M HCl solution (acid hydrolysis), 0.2 M NaOH solution (alkaline hydrolysis), ultrapure water (neutral hydrolysis), 0.6% v/v H₂O₂ solution (oxidation) and 0.02 M FeCl₃ solution (oxidation by metallic ions). Samples were kept at room temperature (23 °C) and protected from light.

Quantum mechanics calculations (QMC) of RN104 and its DP

QMC were performed aiming to theoretically investigate RN104 hydrolysis and Fe complexation as a strategy to support experimental findings. Furthermore, electronic structure and properties were useful to propose a potential mechanism of investigated processes. Initially, the structure of RN104 was built and a conformational analysis was performed using OMEGA 3.1.2.2.^{19,20} Subsequently, the obtained minimal energy conformer was submitted to an energy minimization using density functional theory (DFT) employing B3LYP functional²¹ and 6-311g (d,p) basis set.^{22,23} From this result, two different approaches were considered: (i) electronic properties of RN104 were calculated aiming to investigate its reactivity and, (ii) the RN104-Fe complex (in a 2:1 proportion) was built aiming to simulate its UV absorption spectra. Therefore, both approaches were carried out as complement to elucidation of formed DP by hydrolysis

and Fe addition, respectively. Then, the optimized structure of RN104 and its Fe-complex was submitted to another energy minimization and time dependent-DFT (TD-DFT) study using acetonitrile environment simulated by the integral equation formalism variant of polarizable continuum model (IEF-PCM).^{24,25} The simulated UV spectra were calculated using time dependent DFT approach and the 20 most energetic excitation states. All QMC were performed in Gaussian 09 package²⁶ similarly to other previous works.^{27,28} It is important to mention that there are other DFT studies with similar level of theory on the hydrolysis of organic compounds²⁹ and to predict physicochemical and biological properties of drug-like compounds.^{30,31} As recommended by the literature, 6-311g (d,p) basis set was chosen due to the polarization functions responsible for describe heteroatoms and hydrogen influence on the electronic structure. Lastly, although there are other functionals most indicated to metal complexes calculations (e.g., M06), the major interest in current work is UV-Vis absorption spectra rather than metal bond lengths and angles. The combination of B3LYP functional and 6-311g (d,p) basis set was used due to the ability to predict both electronic structure and properties as well as the UV-Vis absorption spectra in agreement with experimental data.^{32,33}

Results

Analytical method development

The concentration of RN104 optimized for the method was 200 $\mu\text{g mL}^{-1}$. Initially, mobile phase composed

of acetonitrile and water (80:20) was tested at a flow rate of 1.0 mL min^{-1} , injection volume of 25 μL and column temperature at 30 $^{\circ}\text{C}$. Under this condition, the chromatographic profile and the UV spectrum in the range from 200 to 400 nm were verified. The wavelength at 240 nm was selected for RN104 detection. Using the initial conditions, RN104 presented retention time of 10 min. Then, changes were made to the chromatographic conditions to decrease the run time and solvent consumption. By changing the flow rate to 1.2 mL min^{-1} and the mobile phase to acetonitrile and water (85:15), the retention time was 5.9 min. Under these optimized conditions, the method was able to solve RN104 (*Z*) and (*E*) isomers (Figure 2). The thiosemicarbazones derived from aldehydes, such as intermediate compound for RN104 synthesis, tend to form preferentially *E* isomer, thermodynamically more stable. Through the validated method, this observation could be confirmed, since the RN104 solutions presented about 94% of *E* isomer and 6% *Z* isomer.

Method validation

Linear correlations were found between the peak areas and the concentrations of RN104 in the assayed range of the method. The statistical model used was OLSM ($y = 66.488x - 29.771$), the coefficient of determination (r^2) was 0.9999, while the coefficient of correlation (r) was 0.9979. Some basic assumptions were tested and the first one was outlier test using the Jackknife method. After the elimination of the outlier, the demonstration of the normality of the residues was performed applying the

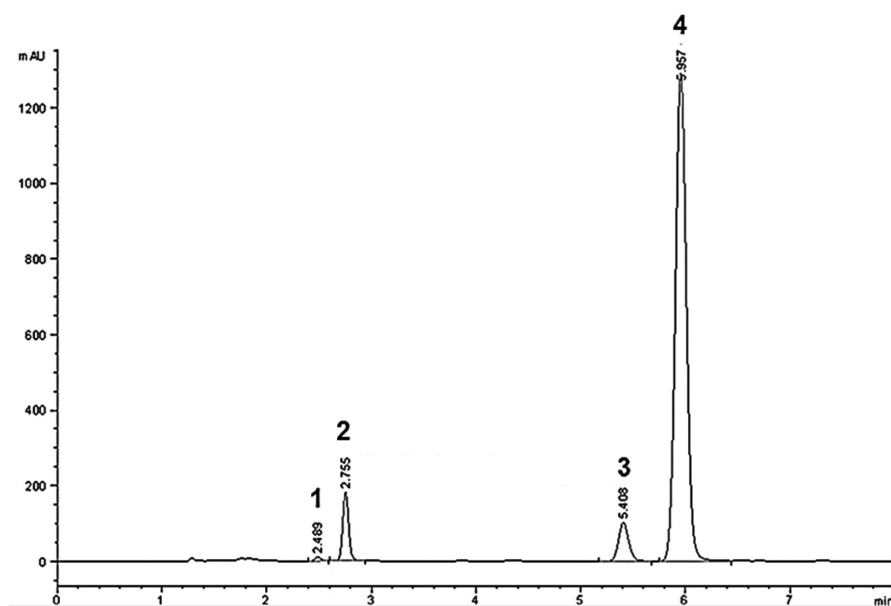


Figure 2. Chromatogram obtained from the injection of the mixture of RN104 and the intermediate product of the synthesis 1 and starting material 2. 1: RN103, $t_R = 2.48$ min; 2: 2-bromoacetophenone, $t_R = 2.75$ min; 3: RN104 (*Z*), $t_R = 5.41$ min; 4: RN104 (*E*), $t_R = 5.95$ min.

Ryan-Joiner method; the independence of the residues by the Durbin-Watson method and the homoscedasticity of the residues by Brown-Forsythe method. Moreover, regression significance and absence of deviation from linearity were confirmed by ANOVA ($\alpha = 0.05$).^{14,15}

In the intra-day precision, the determined mean content was 92.4%, and RSD = 1.3%. For the inter-day precision, the mean content was 92.6% and RSD = 1.3%. Thus, according to the criteria established by the Association of Official Analytical Chemists (AOAC), the developed method may be considered precise, since RSD \leq 2.7% was obtained.¹⁶

The accuracy results are shown in Table 1. Recovery rates between 99.7 and 103.4% and RSD 2.0% indicated that the developed method presented adequate accuracy for the quantification of RN104.¹⁶

The calculated LOD and LOQ were 0.45 and 1.21 $\mu\text{g mL}^{-1}$, respectively. When sequential dilutions of a RN104 solution were performed, the experimental LOD and LOQ were 0.17 and 0.72 $\mu\text{g mL}^{-1}$, respectively. The LOD and LOQ values found based on the signal-to-noise ratio were considerably lower than those calculated by the curve equation and closer to the actual values, since they were obtained from the diluted solution response. These values show that the validated method presents adequate sensitivity to quantify RN104 in the proposed concentration range.

Spectral purity of RN104 chromatographic peak was attested, since the purity angle was smaller than the threshold angle, showing that no interfering products elute at the same retention time of the compound. The developed and validated method was also able to separate and identify the starting materials and intermediate product of synthesis⁴ (Figure 2).

The assayed analytical parameters and the obtained results are shown in Table 2.

According to the obtained values, it can be observed that the developed chromatographic method is robust in relation to the RN104 content when some variations were induced, since the highest variation was 1.5%, when the

Table 1. Accuracy results for the quantitation of RN104 using the HPLC-DAD method

Level	Recovery / %	Recovery mean / %	RSD / %
Low (20 $\mu\text{g mL}^{-1}$)	101.4	103.4	1.7
	104.4		
	104.4		
Middle (120 $\mu\text{g mL}^{-1}$)	99.9	99.7	0.6
	100.2		
	99.0		
High (240 $\mu\text{g mL}^{-1}$)	100.7	100.1	1.1
	100.7		
	98.8		
Mean	–	101.0	2.0

RSD: relative standard deviation.

brand of chromatographic column was changed. Besides the content, the variation of the retention time, the symmetry of the peak, the number of theoretical plates and the resolution were also evaluated. Regarding the retention time, the proportion of the mobile phase was the variable that presented higher impact, since reducing the proportion of acetonitrile decreases the eluent strength, leading to an increase in retention time of RN104 (from 5.9 to 7.6 min). The symmetry of RN104 peak was mostly compromised when changing the brand of the chromatographic column, due to the lower efficiency of varied column.

Forced degradation study

Initially, RN104 degradation tests were carried out under drastic conditions, employing high concentrations of degrading agents. Spectral purity of RN104 chromatographic peak was attested during the method validation and over the degradation study. Longer analytical runs (30 min) were assessed at each degradation condition; however, all formed DP were eluted until 10 min. Analyzes were performed at 24, 48 and 72 h and the results are shown in Table 3.

Table 2. Impact of variations in the analytical parameters on the RN104 content in the robustness validation

Parameter	Nominal and variable	Influence in the percentage content ($X - x$) ^a
Detection wavelength / nm	A = 240; a = 260	0.99
Column temperature / °C	B = 30; b = 35	-0.63
Mobile phase flow rate / (mL min^{-1})	C = 1.2; c = 1.0	-0.51
Mobile phase composition	D = 85:15; d = 80:20	0.34
Brand of chromatographic column	E = Macherey Nagel; e = Merck	-1.46
Brand of acetonitrile	F = Lichrosolv Merck; f = PRQUÍMIOS	-0.38
Chromatograph model	G = Agilent 1100; g = Agilent 1200	-0.50

^aDifference in RN104 content (%) between nominal and varied condition.

Table 3. Degradation of RN104 in forced degradation study

Condition	Degradation / %		
	24 h	48 h	72 h
NaOH (1 M), 23 °C	100.0	100.0	100.0
NaOH (1 M), 50 °C	100.0	100.0	100.0
HCl (1 M), 23 °C	46.3	46.5	46.6
HCl (1 M), 50 °C	69.2	67.3	71.5
Water, 23 °C	12.8	18.2	22.0
Water, 50 °C	27.9	31.0	33.2
Light, 23 °C	1.5	12.8	19.3
Dry heat (105 °C)	10.8	12.3	12.0
H ₂ O ₂ (0.3% v/v), 23 °C	100.0	100.0	100.0
FeCl ₃ (0.01 M), 23 °C	100.0	100.0	100.0

For the acid and alkaline hydrolysis at 50 °C and at room temperature (23 °C) the degradation of compound RN104 was higher than the recommended percentage of up to 30%.³⁴ RN104 undergoes neutral hydrolysis at both tested temperatures, but with a lower extension than the acid and alkaline hydrolysis. The degradation products formed in alkaline hydrolysis are exclusive to this pathway, while those from acid and neutral hydrolysis seem to be similar (Figure 3).

The results of photolytic and thermolytic studies indicated that RN104 is sensitive to light and heat, since the degradation resulting from both conditions was higher than 10% after 72 h.³⁴ For these conditions, there was no formation of a major DP observed in the chromatograms. RN104 was completely degraded in oxidative conditions

and in the presence of metallic ions. In spite of an intense RN104 degradation was found, no additional peak corresponding to degradation products was observed in chromatograms under these conditions.

The stability-indicating method was developed and validated considering the worst case, in which there is the formation of several DP aiming to prove that the method would be able to separate these substances from the main compound.

In order to establish a more realistic degradation profile of RN104, degradation kinetics during 12 h were performed at room temperature, with lower concentrations of the degrading agents. For kinetics of acid and alkaline hydrolysis, the concentrations of degrading agents were reduced from 1 to 0.1 M. Both conditions showed a significant decrease in the concentration of RN104 over time, but alkaline hydrolysis showed to be more intense than the acid. After 12 h, RN104 presented degradation of 20.8% in the acid medium and of 80.6% in alkaline medium. At the same time interval, RN104 was not degraded in water (neutral hydrolysis), since its concentration remained above 98%. The graphs demonstrating the degradation (%) and content (%) of RN104 during 12 h are presented in Figure 4.

For all hydrolytic conditions, the reactions followed a first-order kinetics, in which the rate of degradation depends on the concentration of the reactants. The degradation rate constant (K_{deg}) was calculated from the equation $-K/2.303 = a$, where a is the slope of the line obtained from the natural logarithm of the RN104

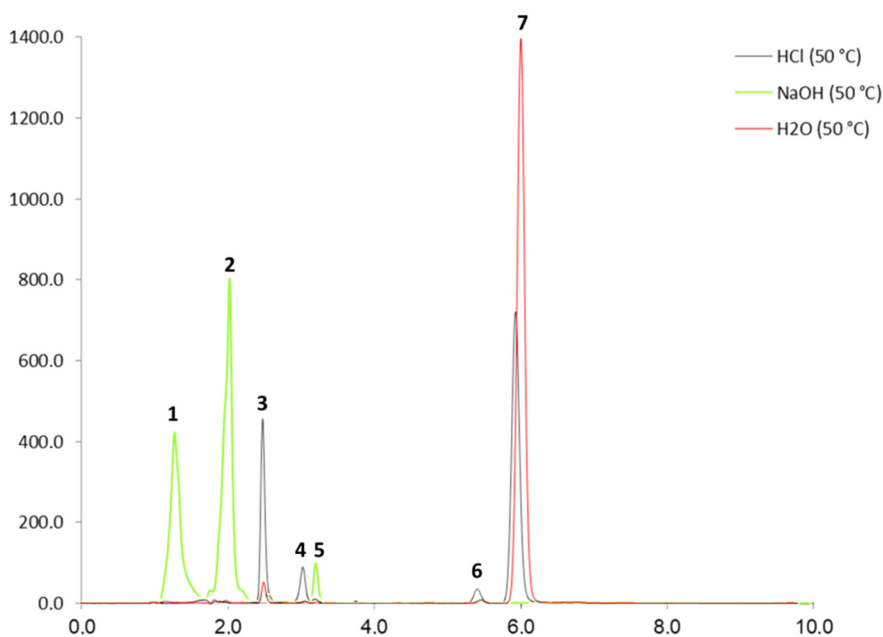


Figure 3. Chromatogram of RN104 under hydrolytic conditions at 50 °C, after 72 h. Black line: acid hydrolysis (1 M HCl); green line: basic hydrolysis (1 M NaOH); red line: neutral hydrolysis. RN104 retention time = 6.0 min. Peaks 1-5: degradation products formed at hydrolytic conditions; peaks 6 and 7: RN104 Z and E isomers, respectively.

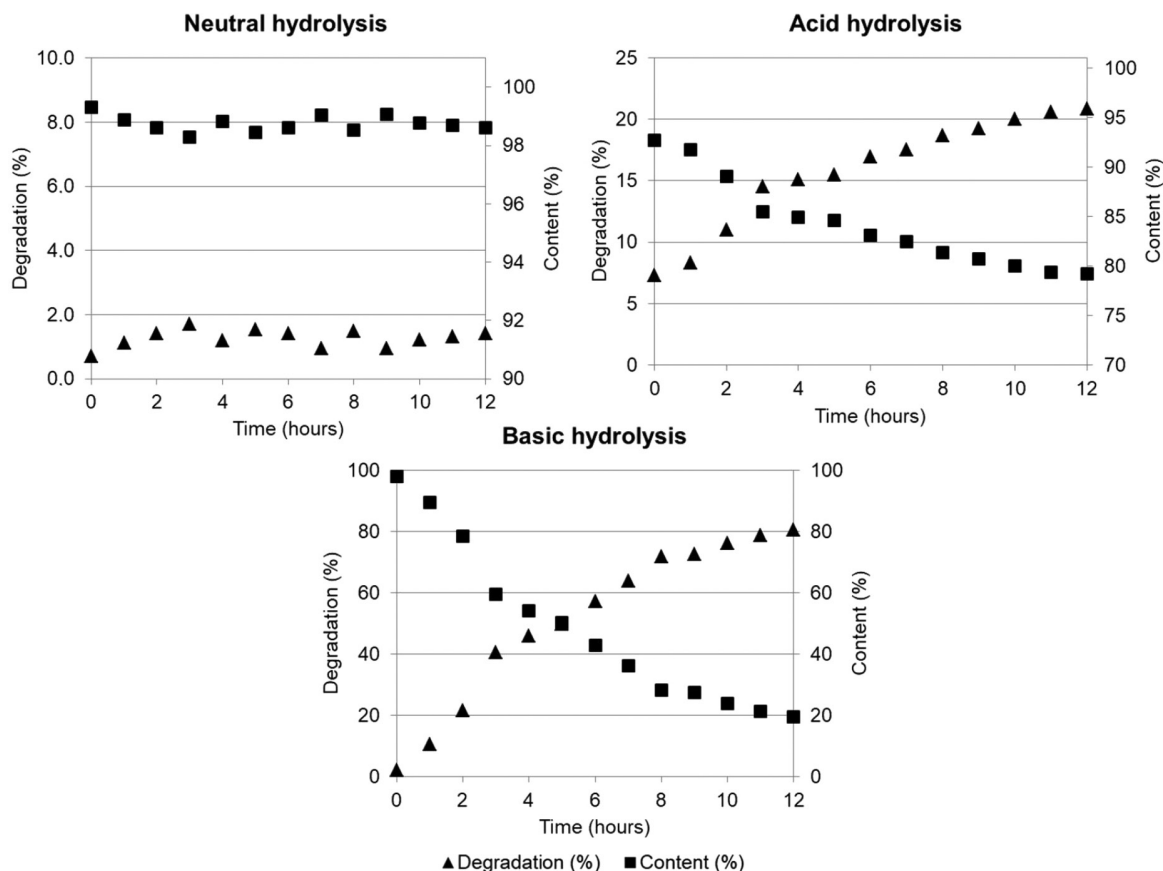


Figure 4. Hydrolysis condition (H_2O , 0.1 M HCl and 0.1 M NaOH) graphs demonstrating content (%) and degradation (%) of RN104 during 12 h.

concentration ($\ln C$) versus time (hours).³⁵ The neutral hydrolysis presented the lowest K_{deg} , corresponding to 0.0015 h^{-1} , whereas alkaline hydrolysis showed the highest value (0.0627 h^{-1}). K_{deg} obtained for acid hydrolysis was 0.0047 h^{-1} .

Since in the initial evaluation of oxidative conditions by H_2O_2 (0.3% v/v) and metallic ions (FeCl_3 , 0.01 M) we could not detect the peak of RN104, the exposure time of the compound was reduced for the kinetic study. Then, the

degradation of RN104 by H_2O_2 at the end of the experiment (12 h) was 26.4% (Figure 5). During the analysis process, it was verified that the solution showed a yellow color immediately after the addition of H_2O_2 and it turned orange during the experiment time.

RN104 showed to be very labile to degradation catalyzed by metallic ions (FeCl_3), since immediately after the addition of the degrading agent, the color of the solution was changed (from colorless to red) as well as

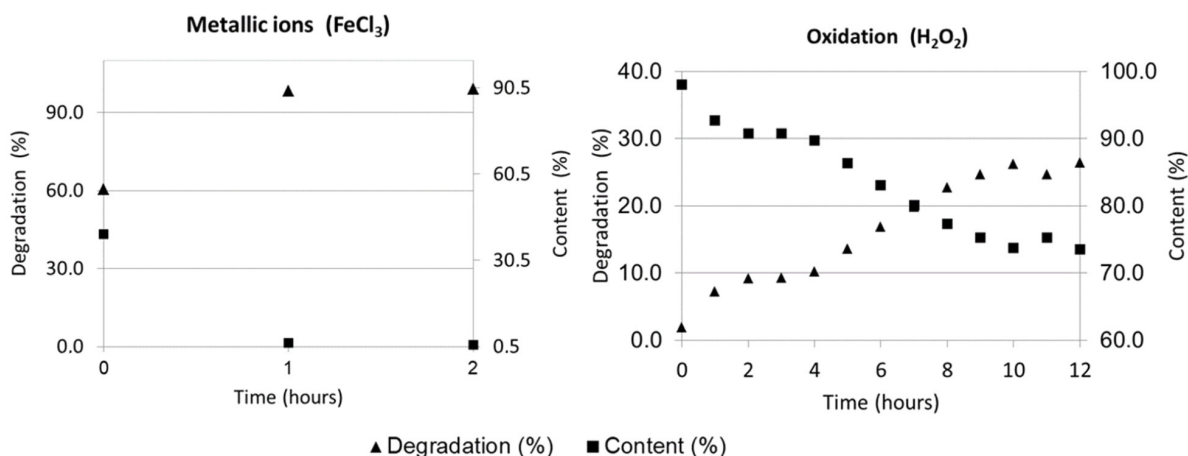


Figure 5. Oxidation (0.3% v/v H_2O_2) and metallic ions (0.01 M FeCl_3) conditions demonstrating content (%) and degradation (%) of RN104 during 12 h.

its odor. The content of RN104 found at the initial time (t_0) was 39.5%, confirming the rapid degradation or even the formation of a complex with Fe^{III} . It was possible to follow the reaction kinetic only until the second hour, since 99.0% of the compound had already been degraded at this time.

QMC of RN104 and its DPs

From electronic structure of RN104, it can be seen that the region of the hydrazone moiety is positively charged (Figures 6a and 6b). Therefore, this is the most favorable region to perform Coulomb interactions with an electron rich group from another molecule (i.e., a nucleophile). Furthermore, the carbon of the hydrazone group has high probability to accept one electron (Figures 6c and 6d). Both results indicate that the attack of a water molecule (nucleophile) on the carbon atom of the hydrazone group is favorable and corroborates the experimental data obtained in this present work and previous results with other thiazolyldiazone derivative studied by our group.³⁶

After energy minimization of RN104, the construction of RN104-Fe complex was done based on the experimental elucidation of other metal(III)-ligand complexes.^{37,38} Two minimized molecules of RN104 were positioned near Fe^{III} atom so that its thiazolyldiazone group interact directly with the metal. After, the built complex structure was also minimized in both vacuum and acetonitrile environments with DFT followed by TD-DFT calculations.

The simulation of RN104 UV-Vis absorption spectra corroborates the experimental spectrum (Figures 7a and 7b) showing two main peaks at 250 and 280 nm.

Discussion

RN104 is a new antifungal with promising activity against *Cryptococcus* spp. and *Candida* spp.³⁻⁵ Considering the potential for the development of RN104-based formulations, the understanding of its intrinsic stability and its impurity profile is essential to allow the production of stable and safe formulations. Degradation products formed during the production or storage of the active ingredient or formulation may decrease the drug potency or may present unexpected pharmacodynamics properties.^{39,40} Therefore, we developed and validated a stability-indicating method for a comprehensive study of RN104 stability and its degradation products.

As RN104 is highly lipophilic, for the development of a stability-indicating HPLC method, different mobile phase compositions containing high proportions of acetonitrile were tested, aiming to avoid the precipitation of the compound in concentrated aqueous solution, as well as high retention times due the strong affinity of RN104 for the C18 stationary phase.

For an analytical method to be also indicative of stability, it has to detect and quantify all DP within a realistic degradation profile. For the development of stability-indicating methods, a complete forced degradation study must be performed to attest the selectivity of the method. The methodology for carrying out the forced degradation tests may vary according to the needs of the study and also the stage of development of the drug.¹¹ Degradation above 30% is not desirable, since drastic conditions lead to the formation of unrealistic DP. Thus, it is not possible to establish if they are identified from the studied compound or if they

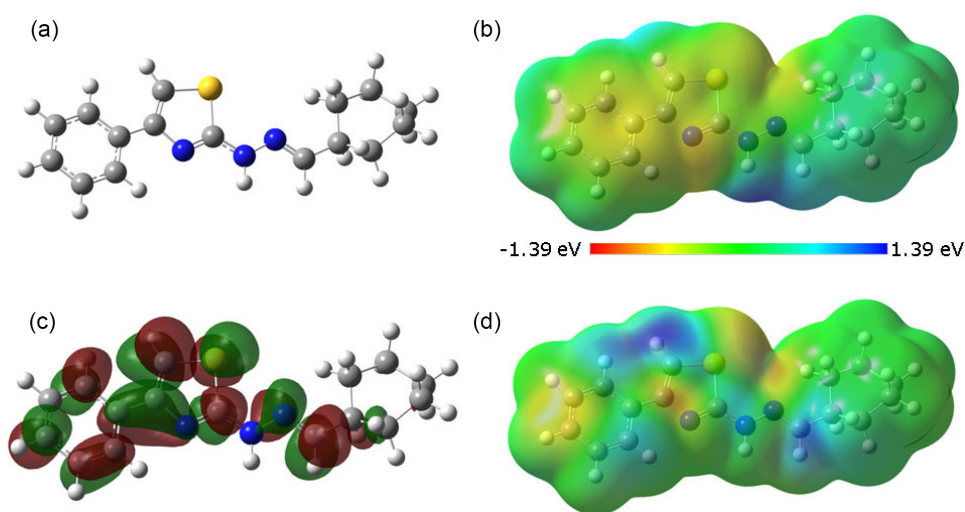


Figure 6. (a) Energy minimized structure of RN104; (b) calculated electrostatic surface potential (ESP) displaying distribution of charges ranging from red (electron rich regions) to blue (electron deficient regions) and passing through green (neutral regions); (c) LUMO map of RN104; (d) LUMO density indicating that red and blue regions have high probability to accept one electron and green low probability of molecular orbital location.

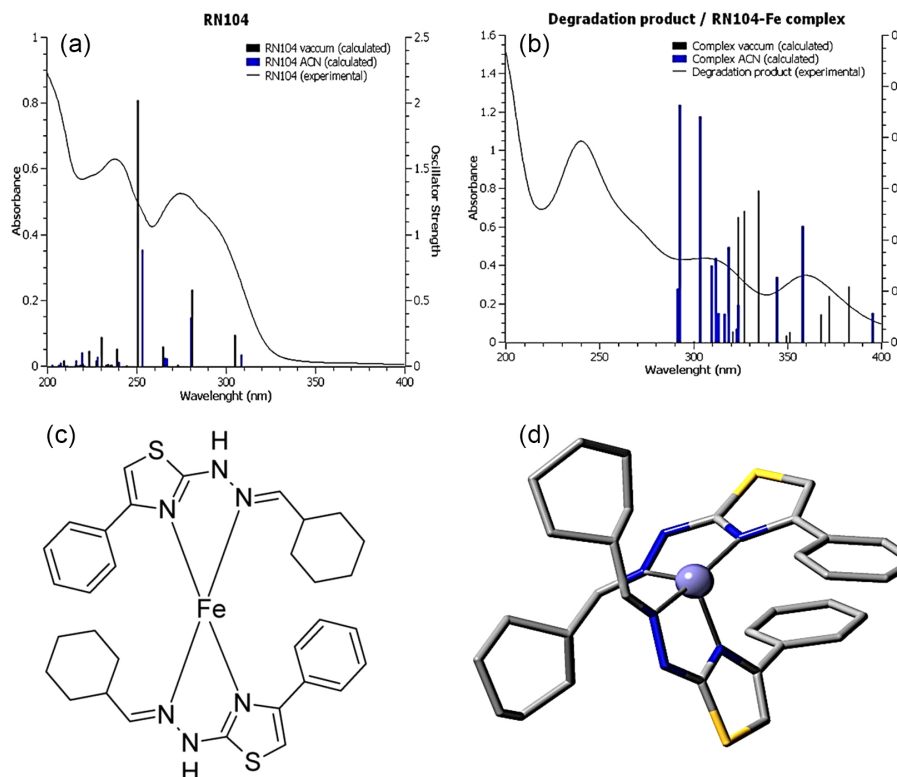


Figure 7. Experimental and theoretical UV absorption spectra for RN104 (a) and formed degradation product in addition to FeCl_3 and Fe-RN104 complex (b). Structure of proposed complex (c) and its 3D optimized structure with DFT method with omitted hydrogen atoms (d).

are by-products of the DP initially formed.³⁴ To attend this recommendation, a degradation kinetics study was carried out during 12 h and performed at room temperature, with lower concentrations of the degrading agents. The forced degradation study indicated that the alkaline hydrolysis and degradation catalyzed by metallic ions (FeCl_3) were the major degradation pathways for RN104. Compounds containing a hydrazone moiety are generally stable under neutral conditions but can easily undergo hydrolysis under alkaline and acid hydrolysis,^{41,42} which is in agreement with what was observed in our study. Based on data from the literature and the results of QMC, we proposed the structures of DP formed from the hydrolysis of RN104 (Figure 8). The cyclohexanecarboxaldehyde formed in this reaction does not have strong UV chromophore and then it would not be detected by the HPLC-DAD method used in

this study. The hydrazone derivative formed may have undergone additional decomposition with formation of low molecular weight products, including NH_3 or N_2 ,⁴³ which would explain why they were not detected under the used analytical conditions.

The formation of metal complexes of hydrazone derivatives and thiazole-based compounds is also described in literature,^{44,45} which demonstrates the consistency of the results obtained from the QMC. Clearly, from the QMC, the simulation of RN104-Fe complex (Figures 7c and 7d) shifted the absorption peaks to red region which is compatible with spectra of formed DP. Furthermore, this peak shift was already described in other works by addition of metal and complex formation.⁴⁶ Therefore, the agreement between experimental and theoretical spectra of RN104 and its complex with Fe^{III} indicated the compatibility of suggested formation of complex in this degradation process.

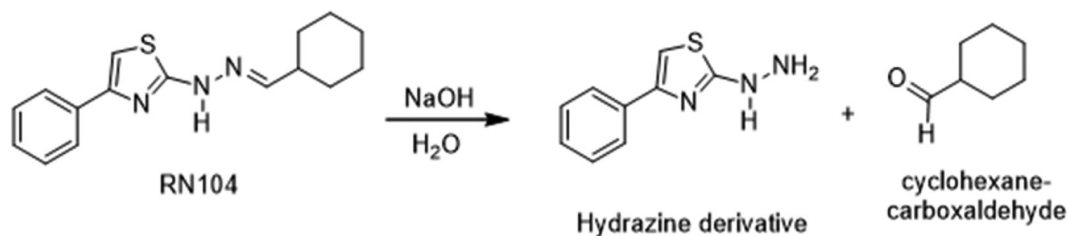


Figure 8. Scheme of the proposed degradation of RN104 in alkaline conditions.

Conclusions

This work contributed to the understanding of the intrinsic stability of compound RN104, a potential candidate for antifungal drug. We developed and fully validated a stability-indicating HPLC method for the quantification of RN104. The forced degradation study allowed evaluating the stability of the RN104 under different conditions. From this study, it was demonstrated that the RN104 is highly sensitive to alkaline hydrolysis and oxidative conditions, and the theoretical elucidation of the major degradation products formed at these conditions was performed by means of quantum mechanics calculations. Thus, for future planning of a formulation, it will be possible to avoid incompatibilities with excipients, packaging materials and manufacturing technology, ensuring the stability of formulation, as well as its safety and efficacy.

Acknowledgments

The authors would like to thank to Professor Dr William R. Rocha and Aline Bozzi of Laboratory of Computational Studies on Molecular Systems from Federal University of Minas Gerais for Gaussian 09 License and the use of computers as well as OpenEye Scientific Software for OMEGA academic license.

This work was supported by Conselho Nacional de Desenvolvimento Científico e Tecnológico (CNPq) and Fundação de Amparo à Pesquisa do Estado de Minas Gerais (FAPEMIG).

References

1. Robbins, N.; Wright, G. D.; Cowen, L. E.; *Microbiol. Spectrum* **2016**, *4*, 903. [Crossref]
2. Pfaller, M. A.; *Am. J. Med.* **2012**, *125*, S3. [Crossref]
3. de Sá, N. P. D.; de Lima, C. M. D.; Lino, C. I.; Barbeira, P. J. S.; Baltazar, L. D. M.; Santos, D. A.; de Oliveira, R. B.; Mylonakis, E.; Fuchs, B. B.; Johann, S.; *Antimicrob. Agents Chemother.* **2017**, *61*, e02700-16. [Crossref]
4. de Sá, N. P. D.; Lino, C. I.; Fonseca, N. C.; Borelli, B. M.; Ramos, J. P.; Souza-Fagundes, E. M.; Rosa, C. A.; Santos, D. A.; Oliveira, R. B.; Johann, S.; *Eur. J. Med. Chem.* **2015**, *102*, 233. [Crossref]
5. Sá, N. P.; Lima, C. M.; dos Santos, J. R.; Costa, M. C.; de Barros, P. P.; Junqueira, J. C.; Vaz, J. A.; Oliveira, R. B.; Fuchs, B. B.; Mylokani, E.; Rosa, C. A.; Santos, D. A.; Johann, S.; *Future Sci. OA* **2018**, *4*, FSO305. [Crossref]
6. Silva, I. R.; Braga, A. V.; Glória, M. B. A.; Machado, R. R.; César, I. C.; Oliveira, R. B.; *J. Chromatog. B* **2020**, *1149*, 122180. [Crossref]
7. Tonholo, D. R.; Maltarollo, V. G.; Kronenberger, T.; Silva, I. R.; Azevedo, P. O.; Oliveira, R. B.; Tagliati, C. A.; *Chem.-Biol. Interact.* **2020**, *315*, 108896. [Crossref]
8. Bajaj, S.; Singla, D.; Sakhuja, N.; *J. Appl. Pharm. Sci.* **2012**, *2*, 129. [Crossref]
9. ICH Q1A(R2); *Stability Test of New Drug Substances and Products*; International Conference on Harmonisation/IFPMA: Geneva, 2003.
10. Food and Drug Administration (FDA); *Guidance for Industry: Analytical Procedures and Methods Validation*; Food and Drug Administration: Rockville, 2015. [Link] accessed in October 2022
11. Agência Nacional de Vigilância Sanitária (ANVISA); Guia No. 4 (1), *Guia para Obtenção do Perfil de Degradação, e Identificação e Qualificação de Produtos de Degradação em Medicamentos*; Agência Nacional de Vigilância Sanitária Ministério da Saúde: Brasília, 2015. [Link] accessed in October 2022
12. Bakshi, M.; Singh, S.; *J. Pharm. Biomed. Anal.* **2002**, *28*, 1011. [Crossref]
13. Minakata, D.; Coscarelli, E.; *Molecules* **2018**, *23*, 539. [Crossref]
14. Agência Nacional de Vigilância Sanitária (ANVISA); Resolução da Diretoria Colegiada (RDC) No. 166, Dispõe sobre a *Validação de Métodos Analíticos e outras Providências*; Diário Oficial da União (DOU), Brasília, No. 141, de 24/07/2017. [Link] accessed in October 2022
15. de Souza, S. V.; Junqueira, R. G.; *Anal. Chem. Acta* **2005**, *552*, 25. [Crossref]
16. Association of Official Analytical Chemists (AOAC); *International Appendix F: Guidelines for Standard Method Performance Requirements*; AOAC: Gaithersburg, 2016. [Link] accessed in October 2022
17. Instituto Nacional de Metrologia (INMETRO); DOQ-CGCRE-008, *Orientação sobre Validação de Métodos Analíticos*; INMETRO: Rio de Janeiro, 2018. [Link] accessed in October 2022
18. ICH Q1B, *Photostability Testing of New Drug Substances and Products*; International Conference on Harmonisation/IFPMA: Geneva, 1996. [Link] accessed in October 2022
19. OMEGA 3.1.2.2; OpenEye Scientific Software, Santa Fe, NM, USA. [Link] accessed in October 2022
20. Hawkins, P. C. D.; Skillman, A. G.; Warren, G. L.; Ellingson, B. A.; Stahl, M. T.; *J. Chem. Inf. Model.* **2010**, *50*, 572. [Crossref]
21. Becke, A. D.; *J. Chem. Phys.* **1993**, *98*, 5648. [Crossref]
22. McLean, A. D.; Chandler, G. S.; *J. Chem. Phys.* **1980**, *72*, 5639. [Crossref]
23. Raghavachari, K.; Binkley, J. S.; Seege, R.; Pople, J. A.; *J. Chem. Phys.* **1980**, *72*, 650. [Crossref]
24. Miertuš, S.; Scrocco, E.; Tomasi, J.; *Chem. Phys.* **1981**, *55*, 117. [Crossref]

25. Cossi, M.; Barone, Cammi, R.; Tomasi, J.; *Chem. Phys.* **1996**, 255, 327. [Crossref]
26. Frisch, M. J.; Trucks, G. W.; Schlegel, H. B.; Scuseria, G. E.; Robb, M. A.; Cheeseman, J. R.; Scalmani, G.; Barone, V.; Petersson, G. A.; Nakatsuji, H.; Li, X.; Caricato, M.; Marenich, A.; Bloino, J.; Janesko, B. G.; Gomperts, R.; Mennucci, B.; Hratchian, H. P.; Ortiz, J. V.; Izmaylov, A. F.; Sonnenberg, J. L.; Williams-Young, D.; Ding, F.; Lipparini, F.; Egidi, F.; Goings, J.; Peng, B.; Petrone, A.; Henderson, T.; Ranasinghe, D.; Zakrzewski, V. G.; Gao, J.; Rega, N.; Zheng, G.; Liang, W.; Hada, M.; Ehara, M.; Toyota, K.; Fukuda, R.; Hasegawa, J.; Ishida, M.; Nakajima, T.; Honda, Y.; Kitao, O.; Nakai, H.; Vreven, T.; Throssell, K.; Montgomery Jr., J. A.; Peralta, J. E.; Ogliaro, F.; Bearpark, M.; Heyd, J. J.; Brothers, E.; Kudin, K. N.; Staroverov, V. N.; Keith, T.; Kobayashi, R.; Normand, J.; Raghavachari, K.; Rendell, A.; Burant, J. C.; Iyengar, S. S.; Tomasi, J.; Cossi, M.; Millam, J. M.; Klene, M.; Adamo, C.; Cammi, R.; Ochterski, J. W.; Martin, R. L.; Morokuma, K.; Farkas, O.; Foresman, J. B.; Fox, D. J.; *Gaussian 09, Rev A.02*; Gaussian, Inc., Wallingford, CT, 2009.
27. Kenawi, I. M.; *J. Mol. Struct.* **2005**, 754, 61. [Crossref]
28. Paulsen, H.; Grünsteudel, H.; Meyer-Klaucke, W.; Gerdan, M.; Grünsteudel, H. F.; Chumakov, A. I.; Trautwein, A. X.; *Eur. Phys. J.* **2001**, 23, 463. [Crossref]
29. Yildiz, I.; *J. Phys. Chem. A* **2016**, 120, 3683. [Crossref]
30. Arslan, E.; Findik, B. K.; Aviyente, V.; *J. Comput.-Aided Mol. Des.* **2020**, 34, 463. [Crossref]
31. Maltarollo, V. G.; de Resende, M. F.; Kronenberger, T.; Lino, C. I.; Sampaio, M. C. P. D.; Pitta, M. G. D. R.; Rêgo, M. J. B. D. M.; Labanca, R. A.; de Oliveira, R. B.; *J. Mol. Graphics Modell.* **2019**, 86, 106. [Crossref]
32. Trossini, G. H. G.; Maltarollo, V. G.; Garcia, R. D.; Pinto, C. A.; Velasco, M. V.; Honorio, K. M.; Baby, A. R.; *J. Mol. Model.* **2015**, 21, 319. [Crossref]
33. Garcia, R. D. A.; Maltarollo, V. G.; Honório, K. M.; Trossini, G. H.; *J. Mol. Model.* **2015**, 21, 150. [Crossref]
34. Baertschi, S. W.; Alsante, K. M.; Reed, R. A.; *Pharmaceutical Stress Testing: Predicting Drug Degradation*, 2nd ed.; Informa Healthcare: London, UK, 2011.
35. Rizwan, M.; Aqil, M.; Azeem, A.; Sultana, Y.; Talegaonkar, S.; Ali, A.; *Chromatographia* **2009**, 7, 1283. [Crossref]
36. Franco, P. H. C.; Vieira, J. G.; Ramos, C. A. D. O.; Johann, S.; de Oliveira, R. B.; César, I. C.; *Biomed Chromatogr.* **2021**, 35, e5014. [Crossref]
37. Miao, S. B.; Ji, B. M.; Zhou, L.; *Synth. React. Inorg., Met.-Org., Nano-Met. Chem.* **2013**, 43, 1296. [Crossref]
38. Kowol, C. R.; Berger, R.; Eichinger, R.; Roller, A.; Jakupec, M. A.; Schmidt, P. P.; Keppler, B. K.; *J. Med. Chem.* **2007**, 50, 1254. [Crossref]
39. Blessy, M. R. D. P.; Patel, R. D.; Prajapati, P. N.; Agrawal, Y. K.; *J. Pharm. Anal.* **2014**, 4, 159. [Crossref]
40. Rao, R. N.; Nagaraju, V.; *J. Pharm. Biomed. Anal.* **2003**, 33, 335. [Crossref]
41. Kalia, J.; R. Raines, T.; *Angew. Chem., Int. Ed.* **2008**, 47, 7523. [Crossref]
42. Singh, N.; Ranjana, R.; Kumari, M.; Kumar, B.; *Int. J. Pharm. Clin. Res.* **2016**, 8, 162. [Crossref]
43. Nemoto, T.; Lazoura, E.; Nomoto, T.; *Chem. Pharm. Bull.* **2003**, 51, 346. [Crossref]
44. Aly, S. A.; Fathalla, S. K.; *Arabian J. Chem.* **2020**, 13, 3735. [Crossref]
45. Frija, L. M. T.; Pombeiro, A. J. L.; Kopylovich, M. N.; *Coord. Chem. Rev.* **2016**, 308, 32. [Crossref]
46. Jia, Z.; Wei, J.; Ren, Y.; Zhang, N.; Hao, X.Q.; Zhu, X.; Xu, Y.; *J. Iran Chem. Soc.* **2020**, 17, 609. [Crossref]

Submitted: June 29, 2022

Published online: October 20, 2022

